Published in final edited form as:
Eur J Pharm Sci. 2011 September 18; 44(1-2): 57–67. doi:10.1016/j.ejps.2011.06.007.

Engineering Tenofovir Loaded Chitosan Nanoparticles:

To Maximize Microbicide Mucoadhesion

Jianing Meng[a], **Timothy F. Sturgis**[b], and **Bi-Botti C. Youan**[a,*]

[1]Laboratory of Future Nanomedicines and Theoretical Chronopharmaceutics, Division of Pharmaceutical Science, University of Missouri-Kansas City, Missouri 64108

[2]Department of Environmental Health and Safety, University of Missouri-Kansas City, Missouri 64110

Abstract

The objective of this study was to engineer a model anti-HIV microbicide (Tenofovir) loaded chitosan based nanoparticles (NPs). Box-Behnken design allowed to assess the influence of formulation variables on the size of NPs and drug encapsulation efficiency (EE%) that were analyzed by dynamic light scattering and UV spectroscopy, respectively. The effect of the NPs on vaginal epithelial cells and *Lactobacillus crispatus* viability and their mucoadhesion to porcine vaginal tissue were assessed by cytotoxicity assays and fluorimetry, respectively. In the optimal aqueous conditions, the EE% and NPs size was 5.83% and 207.97nm, respectively. With 50% (v/v) ethanol/water as alternative solvent, these two responses increased to 20% and 602 nm, respectively. Drug release from medium (281 nm) and large size (602 nm)-sized NPs fitted the Higuchi (r^2=0.991) and first-order release (r^2=0.999) models, respectively. These NPs were not cytotoxic to both the vaginal epithelial cell line and *Lactobacillus* for 48 hours. When the diameter of the NPs decreased from 900 nm to 188 nm, the mucoadhesion increased from 6% to 12%. However, the combinatorial effect of EE% × mucoadhesion for larger size NPs was the highest. Overall, large-size, microbicide loaded chitosan NPs appeared to be promising nanomedicines for the prevention of HIV transmission.

Keywords

Chitosan nanoparticles; HIV prevention; Mucoadhesion; Tenofovir; Vaginal drug delivery

1. Introduction

As one of the most promising drug delivery systems, polymeric nanoparticles (NPs) have been studied extensively and intensively in recent years (Duan et al., 2010). Several polymeric nanoparticulate systems have been prepared and characterized based on both natural and synthetic polymers. Among these polymers, chitosan attracts considerable attention because of its applicable physicochemical and biological properties (Hamidi et al., 2008; Zhang and Kawakami, 2010).

Chitosan is a water-soluble, linear aminopolysaccharide, which is composed of 2-amino-2-deoxy-β-D-glucan combined with glycosidic linkages (Sun et al., 2010). It can be obtained by the deacetylation of chitin, which is one of the most abundant natural polysaccharides found in the exoskeletons of crustaceans, such as shrimp and lobster (Nasti et al., 2009).

*Corresponding author: Tel: 816-235-2410; Fax: 816-235-5779.

Chitosan exhibits many advantages in developing nanoparticles, including biocompatibility, biodegradability, and low-immunogenicity (Agnihotri et al., 2004; Pandey et al., 2005). The high positive charge density also confers its mucoadhesive properties (Plapied et al., 2010), and make it an ideal candidate for the delivery of drugs to mucosal tissues (Sayin et al., 2009). Chitosan also has a very low toxicity. Its LD_{50} in laboratory mice is 16 g/kg body weight, which is close to sugar and salt (Agnihotri et al., 2004).

In comparison with many other polymers, the chitosan backbone contains a number of free amine groups, which makes it used extensively in drug delivery applications. In an acidic environment, the amino groups could be positively charged after protonation. Therefore, chitosan is able to interact with negatively charged molecules (Calvo et al., 1997). Sodium tripolyphosphate (TPP) is a polyvalent anion with three negatively charged phosphate groups. This property enables it to work as a cross linking agent of chitosan. NPs could form spontaneously in mixed TPP and chitosan solutions through inter and intra molecular linkages created between TPP phosphates and chitosan amino groups (Calvo et al., 1997). These types of nanoparticulate systems have shown a high affinity for the association of negatively charged macromolecules (Mohammadpourdounighi et al., 2010), such as the mucin that are present on the mucosal surface.

Tenofovir, which is a nucleotide analogue reverse transcriptase inhibitor, was approved for the treatment of HIV infections by the US Food and Drug Administration in October 2001. Numerous formulations of tenofovir have been prepared to prevent the male to female sexual transmission of HIV, such as gel and the intravaginal ring (Abdool Karim et al., 2010; Johnson et al., 2010). In order for HIV to be incorporated into the host's genomic DNA, a copy of viral RNA must be made, which is facilitated by reverse transcriptase. Tenofovir inhibits enzyme activity by attaching to its active site, subsequently disabling the binding of the natural substrate deoxyadenosine 5'-triphosphate. Once tenofovir is inserted into the viral DNA, the normal 5' to 3' links are prevented from occurring, resulting in HIV DNA chain termination (Grim and Romanelli, 2003). The effect of tenofovir to prevent HIV infection has been provided by previous report (Anderson et al., 2010; Rohan et al., 2010). Tenofovir is a water-soluble, small-molecule drug, which contains a phosphate group and is negatively charged in a NaOH solution. It can also interact with chitosan through electrostatic forces. Chitosan nanoparticles could offer a controlled release drug delivery system for tenofovir.

Recently, tenofovir loaded solid lipid nanoparticles has been engineered for potential intracellular delivery of microbicide using cell penetrating ligands to outdistance the virus (Alukda et al., 2011). In addition to this promising concept, it may be desirable to enhance or maximize microbicides mucoadhesion (3Ms concept) using mucoadhesive ingredients such as chitosan as matrix with the goal of longer retention time and effect to improve patient adherence. The use of complexation between oppositely charged macromolecules to prepare chitosan NPs has attracted much attention. This technique has been previously adapted for the encapsulation of peptides and proteins (Calvo et al., 1997). This study aims for the preparation of tenofovir loaded NPs through the ionic cross-linking of chitosan, which is a kind of physical cross-linking induced by electrostatic interaction. In comparison with chemical cross-linking, it is advantageous because the process is simple and carried out under mild conditions without using hazardous organic solvents (Tiyaboonchai and Limpeanchob, 2007). Thus, it has better biocompatibility than covalently cross-linked chitosan, and it is possible to reduce the potential toxicity (Agnihotri et al., 2004; Park et al., 2010).

2. Materials and methods

2.1. Materials

The chitosan (deacetylation degree of 0.92 and molecular weight of 50–190 *kDa*) and sodium triphosphate pentabasic (TPP) were purchased from Sigma Aldrich (St. Louis, MO, USA). Tenofovir (99% purity) was purchased from Zhongshuo Pharmaceutical Co. Ltd. (Beijing, China). Acetic acid was supplied by Fisher Scientific (Pittsburgh, PA, USA). CytoTox-ONE™ reagent and CellTiter 96® Aqueous One Solution Reagent was purchased from Promega (Madison, WI, USA). All chemicals used in the study were of analytical grade and used as received without further purification.

1.2. Box–Behnken experimental design

A Box–Behnken statistical design with three levels, three factors, and 15 runs was used to design the experiment to optimize the preparation conditions. Some of the polynomial equations relating factors and responses were obtained by Box–Behnken design software (JMP 8, SAS Institute, Cary, North Carolina, USA).

As shows in Table 1, the three key formulation variables (concentration of chitosan, weight ratio of TPP and chitosan, weight ratio of drug and TPP) were represented by X_1, X_2, and X_3, respectively. The evaluated responses (encapsulation efficiency and particle size) were represented by Y_1 and Y_2, respectively (Bei et al., 2009b).

2.3. Preparation of chitosan based NPs

The preparation of chitosan NPs was adapted from a previously described method (Fernandez-Urrusuno et al., 1999). Briefly, chitosan was dissolved in 10 ml of acetic acid (1% v/v) at different concentrations. TPP was dissolved in 1 ml of purified water at various concentrations in order to obtain the final ratio shown in Table 1. The TPP solution was added in a chitosan solution during magnetic stirring at room temperature, spontaneously forming an opalescent suspension.

For the preparation of tenofovir loaded NPs, tenofovir was dissolved in 2 ml of 0.5 M NaOH. Then the drug solution was dropped into the chitosan solution during magnetic stirring, followed by the addition of the TPP solution. The pH of the mixture was adjusted between 5 to 6.5 under continuous stirring for 10 minutes at room temperature.

Chitosan can dissolve in a mixture of acetic acid (1% v/v) and ethanol (Sano et al., 1999). Therefore, in this experiment, beside 1% v/v acetic acid used alone, the solvent mixtures were made of ethanol in 1% acetic acid solution in various ratios (25 and 50%v/v).

NPs were recovered by centrifugation at 20,000 rpm and 20 °C for 60 min (Beckman L8-70 M Ultracentrifuge, Brea, CA, USA). The supernatant was used to determine the drug encapsulation efficiency (EE%). The deposited NPs was washed three times by deionized water, and was freeze-dried (Labconco Corperation, Kansas City, MO, USA) and stored at 4 °C−8 °C.

2.4. Particle size determination

Different NPs samples were resuspended by sonication (Qsonica LLC, Newtown, CT, USA) in distilled water, and the particle size and polydispersity index was determined through dynamic light scattering (Zetasizer Nano ZS, Malvern Instruments Ltd, Worcestershire, UK) at the temperature of 25°C. Samples with PI < 0.05 were considered monodispersed according to the National Institute Standard (Sassi et al., 2008).

2.5. Encapsulation efficiency

The content of tenofovir was calculated from the difference between the total amount of drug added in the NP preparation and the amount of free drug in the supernatants. The amount of unencapsulated drug was measured by UV spectrophotometer (Spectronic Genesys 10 Bio, Thermo Electron Corperation, WI, USA) at a wavelength of 259 nm. The drug EE% was calculated as follows:

$$EE\% = \frac{\text{Total amount of tenofovir} - \text{Free tenofovir}}{\text{Total amount of tenofovir}} \times 100 \quad \text{Eq. 1}$$

2.6. Morphological analysis

The transmission electron microscopy (TEM) was used to assess the morphology of NPs. To obtain the specimens, drops of nanoparticle suspension were placed on a copper grid with a carbon support film and air dried. The NPs were viewed under a Scanning Transmission Electron Microscope CM12 (FEI, Hillsboro, OR, USA) at 80 kV accelerating voltage. Digital images were acquired with an ORIUSTM SC 1000 11 Megapixel CCD camera (Gatan, Pleasanton, CA, USA).

2.7. In vitro release study

Two milliliters of the NP suspension was put into a Spectra/Por cellulose ester membrane dialysis bag (Spectra/Por Float-A-Lyzer G2, MWCO 3.5–5 KD, Spectrum Laboratories Inc. Rancho Dominguze, CA, USA), and immersed into 20 ml of vaginal fluid stimulant (VFS) that was prepared according to previous reports (Owen and Katz, 1999; Sassi et al., 2008). The media was incubated in a thermostatically controlled shaking (60 rpm) water bath (BS-06, Lab Companion, Seoul, Korea) at 37 °C. At predetermined time intervals, all the buffer solution outside the dialysis bag was removed and replaced by fresh buffer solution to maintain a sink condition. The concentration of the drug in the solution was determined by a UV spectrometer at 260 nm. Each experiment was run in triplicate together with a blank.

2.8. Lactate dehydrogenase (LDH) assay

The vaginal epithelial cells were seeded in a 96-well plate. The medium was changed with 100 μl medium with chitosan NPs of different sizes. The concentration of NPs was 1 mg/ml. A medium without NPs was used as negative control, and 1% Triton X was used as positive control. A row of wells without cells was used to determine the background fluorescent that might be present due to media only. The plate was incubated at 37 °C for 4 and 48 hrs, and then equilibrated to 22 °C.

One hundred microliters (100 μl) of CytoTox-ONE™ reagent (Promega, Madison, WI, USA) was added to each well and shaken for 30 seconds. The plate was incubated under 22 °C for 10 min, and then 50 μl of stop solution was added to each well. The fluorescence was determined by a DTX 800 multimode microplate reader (Beckman Coulter, Brea, CA, USA) at an excitation wavelength of 560 nm and an emission wavelength of 590 nm. The percent cytotoxicity of can be expressed as:

$$Cytotoxicity(\%) = \frac{Experimental - Background}{Positive - background} \times 100 \quad \text{Eq. 2}$$

Where Experimental was the absorbance of NP-treated wells, Background was the absorbance of background wells (wells without cells), and Positive was absorbance of positive control wells (cells treated with 1% Triton X).

2.9. MTS assay

Cell viability was determined by adding MTS and then checking the amount of the colored formazan product that was bioreduced from the MTS by the cells. Cells were seeded and incubated with NPs under the same condition as above following the manufacturing protocol. At different intervals, nanoparticle suspension was removed and substituted with fresh medium. Twenty microliters of CellTiter 96® Aqueous One Solution Reagent (Promega, Madison, WI, USA) was added to each well and incubated at 37 °C for 4 hours. The absorbance was recorded at a wavelength of 490 nm.

$$Viablility(\%)=\frac{ABS_{Test}}{ABS_{Control}}\times 100 \quad \text{Eq. 3}$$

Where ABS_{Test} and $ABS_{Control}$ represented the amount of formazan detected in viable cells.

2.10. *Lactobacillus* viability Assay

The *Lactobacillus* viability assay was performed to assess the effect of chitosan NPs on *L. crispatus* growth using the established method (Lackman-Smith et al., 2008). Briefly, the bacteria density was adjusted to an OD_{670} of 0.06, corresponding to a 0.5 McFarland Standard or 10^8 CFU/ml (Klebanoff and Coombs, 1991; Quayle, 2002). *L. crispatus* was plated in a 96-well plate at a volume of 100 μl, and then incubated with 100 μl of 1 mg/ml NP suspension under 37 °C. Commercially available 10 μg/ml of Penicillin-Streptomycin solution (Invitrogen, Carlsbad, CA, USA) was used as positive control. After 4 and 48 hours, 20 μl of MTS reagent was added to each well and the bacterial viability was determined by a microplate reader by measurement of the absorbance at a wavelength of 490 nm. The percent viability can be calculated using the above equation 3.

2.11. Bioadhesion test

Fluorescein isothiocyanate (FITC)-labeled chitosan was synthesized based on the reaction between the isothiocyanate group of FITC and amino group of chitosan (Thongborisute et al., 2006), using the method previously described (Ma and Lim, 2003). Porcine tissue was freshly obtained from the local abattoir (Fairview Farm Meat Co., Topeka, KS, USA) within 2 hours of the death of the animal (Tobyna et al., 1997). The tissue was washed with normal saline, snap-frozen in liquid nitrogen, and kept at −80 °C. When required, the tissue was thawed at 4 °C then brought to room temperature gradually (Jackson and Perkins, 2001) and cut into pieces of 8 cm length and 1 cm width. The outside of the vaginal tissue was stuck to a plastic strip by cyanoacrylate glue, which is resistant to water and harmless to the tissue as previously reported (Grabovac et al., 2005). Then, the tissue-containing strip was immersed into a tube containing FITC labeled NPs (10 mg/ml) in 10 ml of VFS. The tube was put into a shaking water bath for 30 min at 100 rpm, and then removed for analysis of the remaining fluorescence in the VFS (Dudhania and Kosaraju, 2010). The fluorescence of the VFS before and after the treatment was analyzed by a microplate reader at λ_{ex}490 nm and λ_{em}520 nm. The percent mucoadhesion was calculated as follows:

$$Mucoadhesion(\%)=\frac{F_I-F}{F_I}\times 100 \quad \text{Eq. 4}$$

Where F_I was the initial fluorescence and F was the remaining fluorescence of the VFS after the treatment (Dudhania and Kosaraju, 2010).

2.12. Statistics analysis data

All experiments were performed in at least three independent assays. The results were given as mean ±standard error of the mean (SEM). Statistical comparisons of the results to control were made with independent sample t-tests or ANOVA. The level of significance was taken as p value < 0.05.

3. Results and discussions

3.1. Formation and physicochemical characterization of chitosan Nps

Upon addition of TPP, the NPs were formed through the gelation process. The results of the Box-behnken design for EE% (Y_1), average particle size (Y_2), and polydispersity index (PI) are shown in Table 2. The polynomial equations for both response values were:

$$Y_1=4.66+1.12X_1+1.04X_2-1.28X_3+1.58X_1X_2-0.31X_1X_3+0.30X_2X_3-0.16X_1^2-0.18X_2^2-1.17X_3^2 \quad \text{Eq. 5}$$

$$Y_2=187+21.13X_1+0.37X_2+15.94X_3+6.1X_1X_2-3.2X_1X3+26.93X_2X_3-3.99X_1^2+22.99X_2^2+20.50X_3^2 \quad \text{Eq. 6}$$

Equation 5 and 6 show the effect of the independent variables and their influences on the EE % and particle size. The coefficient of interaction terms show how the Y_1 and Y_2 changed when the two independent variables changed simultaneously. The significance of these variables and their interactions are shown in Fig. 1. The values on the x-axis of the Pareto charts represent the standardized effects, which are in fact the ratio of estimate and the standard error of the factor effect (t value) (Vander Heyden et al., 2001). The obtained t value was compared to a tabulated critical t value, which was determined at α=0.05 for residual degrees of freedom (df), where df=5 from ANOVA (Table 3) (Miller and Miller, 1993). The factors whose length passed the vertical line ($t_{critical}$=2.571 at P<0.05) indicated significance on the response value (Bei et al., 2009a). According to Fig. 1, X_3, X_1, X_1X_2, and X_2 contributed substantially to EE% (Fig. 1. A), while X_1 and X_2X_3 contributed to size (Fig. 1. B). Chitosan was used in these nanoformulations as polymeric matrix required to entrap the drug and to allow controlled drug release. The concentration of chitosan (X_1) was found to increase the EE%. By increasing the amount of polymeric matrix (chitosan), more tenofovir could interact with the chitosan through electrostatic forces. TPP was the cross-linking agent. By increasing the weight ratio of TPP/chitosan (X_2), more chitosan molecules, which contain several drug molecules, can participate in the gelation process and form NPs so that more drug can be entrapped into the particles. The interaction factor X_1X_2 was also positively related to the EE% as a result of the above phenomena. The ratio of TPP/chitosan and tenofovir/chitosan was chosen according to the Nitrogen to Phosphate or N/P ratio previously described (Grayson et al., 2006; Woodrow et al., 2009). Briefly, the molar ratio of the amino/phosphate group (N/P ratio) in the solution should be larger than 1:1. A high EE% occurred when the molar ratio of the amino group of chitosan to the phosphate group of drug was 8:1. These values agreed with the results obtained from the BBD design where the ratio of drug/chitosan (X_3) showed a negative effect on the EE%, which meant that the higher the relative amount of drug to polymer in the solution, the lower the percentage of the total drug that can be entrapped in the NPs.

According to Fig. 1 B, the concentration of polymer (X_1) in this study has a positive effect on the nanoparticle size, which agreed with published results (Wu et al., 2009) that larger sized NPs were obtained with higher concentrations of chitosan. However, the mechanism by which X_2X_3 contributed to size increase was not clear, perhaps because TPP and tenofovir (both with phosphate groups) competitively interacted with the same chemical

group of chitosan. Therefore, X_2X_3 interaction might affect the cross-linking efficiency leading loosely packed polymeric chain inside the NPs with increased particle size.

At a medium amount of chitosan the TPP and drug mixture was required to achieve a higher EE% and lower size. Base on the interaction plot shows in Fig. 2 and equations 5 and 6, the optimal formulation, which exhibited the highest EE% (5.83%±0.88%) and lowest particle size (207.97±19.07 nm), was selected through the mathematical optimization process, where X_1, X_2, and X_3 were 0.66, 0.67, and −0.69. Table 3 shows the results from the ANOVA.

A check point analysis base on equation 1 and 2 was performed to confirm; the analysis is shown in Table 4. Three points were selected: two random points out of the 15 runs of the experiment, and the above theoretical and optimal point. Though the Error % on the EE% was large (which might have resulted from the variability in the UV spectroscopy absorbance reader), the differences between measured and predicted values were not found to be statistically significant ($p > 0.05$); thus, it can be concluded that these equations fit the data satisfactorily and were valid for predicting the EE% and the particle size.

At a higher pH, more particles were formed compared to a lower pH because the proportion of the protonated amino groups in chitosan is pH dependent. Chitosan has weak basic amino groups that are protonated in acidic medium. TPP with a negative charge could interact strongly with positively charged chitosan in such a low pH environment (Hu et al., 2010). Another important factor is the degree of deacetylation of chitosan. The higher deacetylation degree of chitosan could provide more free protonable amino groups and lead to a higher EE % (Aranaz et al., 2009). The molecular weight also could influence the physicochemical properties to a significant extent. A small size of nanoparticles could be arrived by using the low molecular weight chitosan (data not shown). A recent report also shown that chitosan exhibit a molecular-weight-dependent negative effect on human cell viability, though the mechanism is not yet fully understood (Wiegand et al., 2010).

However, the EE% of tenofovir was quite low (5.83%), although the preparation was performed at the optimal condition. To improve the EE%, a mixture of ethanol and water was used as a solvent for chitosan. The effects of ethanol concentration on the EE% and the size of NPs are shown in Fig. 3. The predicted water solubility of tenofovir is 1.87 mg/ml and Log P is −1.6 (Van Gelder et al., 1999); thus, the observed low EE% may be explained by the relatively high hydrophilicity (Denkba et al., 2000) and low molecular weight of this drug (MW= 287 Da). To provide a perspective on other low molecular weight molecules encapsulated into chitosan nanoparticles, it is important to underscore that recently, carboplastin (MW= 371 Da) was encapsulated at 20 wt.% using a modified gelation technique (Parveen et al., 2010; Arya et al., 2011). Doxorubicin (MW= 543 Da) was encapsulated at up to 67.9% using electrospray ionization method (Songsurang et al., 2011) suggesting that the investigation of such alternative methods is also warranted in future studies to dramatically improve this drug's EE%. Tenofovir could not dissolve in ethanol, and the addition of ethanol reduced the amount of required water. As a result, the solubility of tenofovir in ethanol was lower than that in water alone. Therefore, the drug could not diffuse out in massive amounts during the nanoparticle preparation, leading to a higher EE% (Yu et al., 2009). Indeed, the EE% with ethanol on the optimal condition was 20.05±3.27% (n=3) (Fig. 2), which was almost three fold higher than that of water alone.

However, the use of ethanol also increased the particle size from 207.97±19.07 nm to 580.60±98.71 nm. The size increase might be explained by the Kelvin equation (equation 7):

$$\ln\frac{p}{p_0}=\frac{2\gamma V_m}{rRT} \qquad \text{Eq. 7}$$

Where p is the actual vapor pressure of the liquid, p_0 is the saturated vapor pressure, γ is the surface tension, V_m is the molar volume, R is the universal gas constant, r is the radius of the droplet, and T is temperature. Rewriting Equation 7 gives:

$$r=\frac{2\gamma V_m}{RT\ln\frac{p}{p_0}} \quad \text{Eq. 8}$$

The surface tension of ethanol (22.8 mN/m) is less than that of water (72.8 mN/m) (Ma and Liu, 2010); thus, ethanol can significantly decrease the surface tension of the chitosan solution. According to Equation 8, the radiuses of the droplets (r) decrease with the decrease in the surface tension when the other equation parameters are fixed, which means that ethanol can lead to smaller droplets.

Even if we assume that γ effect is negligible, another important parameter that describes droplet deformation is the Weber number (W_e):

$$We=\frac{G\eta R}{2\gamma} \quad \text{Eq. 9}$$

Where G is the share stress, η is the viscosity, R is the radius of the droplets, and γ is the interfacial tension (Tadros et al., 2004). Equation 9 can be rewritten as:

$$R=\frac{2We\gamma}{G\eta} \quad \text{Eq. 10}$$

The radius of the droplets decreases with the increase of η. At 25 °C, the viscosity of water is 0.894 cP, while the viscosity of ethanol is 1.074 cP (Lide, 2009–2010), which means that the ethanol addition also leads to smaller droplets.

The initial smaller particles, produced under the influence of either low surface tension or low viscosity induced by ethanol, will undergo Brownian motion and particle collision leading to particle growth. In fact, the growth of aggregates can be simulated by making simple assumptions concerning the transport of particles to the growing agglomerate, and the events which occur when primary particles collide with the growing aggregate. The relationship between mass and final size of the NPs can be defined by a mass-fractal aggregation equation:

$$R=\alpha N^{1/df} \quad \text{Eq. 11}$$

Where α is the lacunarity constant, R is the aggregate overall size, N is the number of primary particles in an aggregate, and d_f is the mass-fractal dimension which ranges from 1 to 3 in a 3-dimensional space. The colliding particles can probe the surface of the growing aggregate, or become “trapped”, by high coordination number regions of the aggregate. According to equation 11, the larger number of colliding droplets leads to the growth of larger droplets, which agreed with the result that the size of the final NPs cured in ethanol solution was relatively larger. Fig. 4 shows the mean size distribution of particles formed in water (Fig. 4. A) and 50% (v/v) ethanol (Fig. 4. B). These size analyses data were consistent with the TEM data (Fig. 5).

3.2. In vitro release study

Drug release from solid dosage form has been described by kinetic models such as zero-order, first order, Higuchi model, Peppas model, and Hixon-Crowell (Costa and Sousa Lobo, 2001). The release data was fitted to zero-order, first order, and the Higuchi model to propose the release mechanism (Bhatt et al., 2008). Table 5 shows the formulation and characteristic of NPs used in the release study. The suspensions are stable, with zeta potential being as high as 45–55mV, which is also close to the results reported in the previous published literature (Wu et al., 2005; Bao et al., 2008; Nasti et al., 2009). The positive charge of NPs is due to the amino groups on the surface of the NPs. The drug release profiles of chitosan NPs are shown in Fig. 6. It was noteworthy that small-sized NPs showed an initial burst release phase within the first 8 hours. Since it is well known that in most of the drug release conditions for the particles, a higher drug loading level generally leads to a higher drug release rate because of the enhanced diffusion driving force of the concentration gradient (Yu et al., 2009). However, in this study the burst release occurred possibly due to the small size of the NPs. As the particle diameter was reduced, the specific surface area increased, while the path length to the surface of the drug decreased (Cordova et al., 2008). It is thus more likely for a drug to be released from the NPs. Medium and large-sized nanoparticles provided a controlled drug release without an obvious burst release. Drug release from medium-sized NPs fit well with the Higuchi model (Costa and Sousa Lobo, 2001):

$$Q=7.15t^{1/2} - 4.04 \quad (r^2=0.991) \qquad \text{Eq. 12}$$

Where Q is the percent of drug released in time t. The high-sized NPs fit with the first-order release model (Costa and Sousa Lobo, 2001):

$$\ln(100 - Q)= - 0.0078t+4.5 \quad (r^2=0.999): \qquad \text{Eq. 13}$$

Both of medium-sized and large-sized NPs could be considered as promising drug nanocarriers for controlled release of the microbicide. The size of NPs appears to be a major factor affecting the drug release rate.

The average daily release of tenofovir from chitosan NPs was 14% (medium) and 12% (large). As the drug loading of the two kinds of particles was 0.33% (w/w) and 1.14% (w/w) (Table 5), 1 mg of nanoparticles could release 0.5×10^{-3} mg and 1.4×10^{-3} mg of drug every 24 hours. Women of reproductive age produce fluid at a rate of approximately 6 ml/day (Baloglu et al., 2009), while the EC_{50} of tenofovir was about 0.5 μM (Balzarini et al., 2002), which means that about 1.7 g of medium size chitosan NPs, or 0.6 g large-size chitosan nanoparticles, would be able to provide the daily requirement of tenofovir for an adult woman patient. This is feasible considering that the average vaginal suppository that could be measured as an additional vehicle had a weight of 5 grams. However, although the below cytotoxicity study has shown that both medium and large sized nanoparticles are not cytotoxic to human vaginal epithelial cells and *Lactobacillus crispatus*, the in vivo safety of these nanoparticles remains to be elucidated in future studies before any clinical use.

3.3. Cytotoxicity studies

Lactate dehydrogenase (LDH) and MTS tests are utilized to evaluate the effect of chitosan NPs on both cellular viability and membrane integrity. The LDH from cells with damaged membranes was determined by measuring the fluorescent signal. NPs used in this study were the same as shown in Table 5, but without drug loading. After incubation with chitosan NPs for 4 and 48 hours, only minimal LDH release from vaginal epithelial cells was

observed. As shown in Fig. 7, the extent of the release of LDH from the cells incubated with NPs was 10% higher than that of media.

The MTS tetrazolium compound is able to be bioreduced by living cells into a colored formazan product that is soluble in the cell culture media. Thus, after the incubation, the number of living cells could be determined by the absorbance of the formazan product of MTS. The viability of cells, which was higher than 80%, is shown in Fig. 8. For some in the sample, the cell viability was even higher than 100% in comparison with the media control, which may be due to the differences of the number of cells in each well.

In both of the assays, no statistical difference was observed by the t-test between media control and NPs with different sizes, which means that the chitosan NPs are not harmful to the cells and the size has no effect on cytotoxicity.

3.4. Effects on viability of *Lactobacillus crispatus*

Lactobacillus, which is a predominant normal vaginal floral species, was used as model bacteria since it is able to produce hydrogen peroxide (H_2O_2) (Wilks et al., 2004). It is critical that any microbicide formulation won't disturb normal vagina flora so that they can maintain a low pH environment and secrete H_2O_2, which provides a natural barrier for HIV transmission (Klebanoff and Coombs, 1991; Quayle, 2002).

As shows in Fig. 9, after incubation for 4 and 48 hrs, there was no statistical difference between the media control and the chitosan NPs, which suggests that these NPs are not harmful to the cells and the size has no effect on cytotoxicity.

3.5. Mucoadhesion studies

Porcine vaginal tissue was used for this study because vaginal mucosa is a realistic and reproducible system to assess the therapeutic potential of new agents in humans (Squier et al., 2008). Chitosan has a well-known bioadhesive property by establishing the electrostatic interactions with sialic groups of mucins in the mucus layer (Ikinci et al., 2002; De Campos et al., 2003; Bravo-Osuna et al., 2007), which is on the surface of the vaginal tissue. After fluorescence tagging, the average diameter of small, medium, and large particles was 188.7±43.3 nm, 273.5±53.1 nm, and 900.2±118.4 nm, respectively. For large-sized NPs, the difference in size may be due to the ethanol use. Chitosan nanoparticles interact with mucins using the amino groups on the surface of nanoparticles. Therefore, it was reasonably speculated that the incorporation of drug would not dramatically change the mucoadhesion behavior of these nanoparticles since the drug is entrapped inside the matrix (Arya et al., 2011). Recently solid lipid nanoparticles have been proposed for actice transport of microbicide into deeper epithelial tissue (Alukda et al., 2011). However, most of the mucoadhesive nanosystem would remain in the mucus layer due to the intimate contact with the mucosa (das Neves et al., 2011) for a relatively longer duration of action. The performance of most drugs could be improved by using bioadhesive carriers, which provide prolonged contact time between the polymeric system and mucous layer surface (Baloglu et al., 2009), and a controlled drug release.. Moreover, it was also demonstrated that chitosan can enhance the absorption of hydrophilic molecules by promoting a structural reorganization of the tight junction-associated proteins (Jung et al., 2000; Leane et al., 2004; Vllasaliu et al., 2010).

The contribution of particle size to the mucoadhesion % of chitosan NPs is shown in Fig. 10. There was no statistical difference between low and medium-sized NPs (P=0.32); however, the mucoadhesion % of large-sized NPs was halved (P value between low and large size NPs was 0.003).

Since the mucoadhesive properties of the NPs are due to the electrostatic attraction between amino groups of chitosan on the surface of the NPs and the sialic acid group of mucin, the total specific surface area was the decisive factor of the mucoadhesion. For small particles, more chitosan molecules have a chance to contact the mucous layer. Thus, the mucoadhesive property of small chitosan NPs was improved. To achieve a desired dosage, both the EE% and mucoadhesion % (MA%) should be considered to efficiently identify the ultimate formulation process. Assuming that for all the three kinds of NPs, drug EE% remains unchanged after fluorescence tagging, the mass fraction of EE% × MA% was found to be 0.26%, 0.99%, and 1.71%, respectively, using the approach in the previous report (Ghaderi and Carlfors, 1997). Though the percent mucoadhesion of large-sized NPs was lower than that of low and medium-sized particles, the mass fractions were higher than that of the other two kinds of particles, which indicated that large-sized chitosan NPs are ultimately the most promising vehicle for preparing chitosan based vaginal or topical microbicide delivery.

4. Conclusion

In this work, reported for the first time, microbicide loaded chitosan NPs were prepared by ionic gelation. The EE% of tenofovir, which was used as a model microbicide, could be improved significantly by using an ethanol solution as a solvent of chitosan. However the use of ethanol also increased the particle size. The *in vitro* release, cytotoxicity assays, and mucoadhesive studies suggested that relatively large chitosan NPs have the potential to be a controlled release, safe, and bioadhesive microbicide delivery system. These properties make chitosan NPs a good candidate for the topical vaginal microbicide delivery system for further study related to the quest of the prevention of HIV transmission.

Acknowledgments

The work presented was supported by Award Number R21A1083092 from the National Institute of Allergy and Infectious Diseases. The content is solely the responsibility of the authors and does not necessarily represent the official view of the National Institute of Allergy and Infectious Diseases or the National Institute of Health. The authors are grateful to Dr. Vladimir M. Dusevich (School of Dentistry, University of Missouri-Kansas City, MO) for the transmission electron microscope. The authors also would like to thank Mrs. Claire Forster (Fairview Farm Meat Co., Topeka, KS,) for kindly providing the fresh porcine vaginal tissue and Margaret LoGiudice, R.D.H., M.S. (Johnson County Community College, Overland Park, KS) for helpful and thorough proof reading of this manuscript.

References

Abdool Karim Q, Abdool Karim SS, Frohlich JA, Grobler AC, Baxter C, Mansoor LE, Kharsany AB, Sibeko S, Mlisana KP, Omar Z, Gengiah TN, Maarschalk S, Arulappan N, Mlotshwa M, Morris L, Taylor D. Effectiveness and safety of tenofovir gel, an antiretroviral microbicide, for the prevention of HIV infection in women. Science. 2010; 329:1168–1174. [PubMed: 20643915]

Agnihotri SA, Mallikarjuna NN, Aminabhavi TM. Recent advances on chitosan-based micro- and nanoparticles in drug delivery. J Control Release. 2004; 100:5–28. [PubMed: 15491807]

Alukda D, Sturgis T, Youan BB. Formulation of tenofovir-loaded functionalized solid lipid nanoparticles intended for HIV prevention. J Pharm Sci. 2011

Anderson PL, Kiser JJ, Gardner EM, Rower JE, Meditz A, Grant RM. Pharmacological considerations for tenofovir and emtricitabine to prevent HIV infection. J Antimicrob Chemother. 2010; 66(2): 240–250. [PubMed: 21118913]

Aranaz I, Mengíbar M, Harris R, Paños I, Miralles B, Acosta N, Galed G, Heras A. Functional Characterization of Chitin and Chitosan. Current Chemical Biology. 2009; 3:203–230.

Arya G, Vandana M, Acharya S, Sahoo SK. Enhanced antiproliferative activity of Herceptin (HER2)-conjugated gemcitabine-loaded chitosan nanoparticle in pancreatic cancer therapy. Nanomedicine. 2011

Baloglu E, Senyigit ZA, Karavana SY, Bernkop-Schnurch A. Strategies to prolong the intravaginal residence time of drug delivery systems. J Pharm Pharm Sci. 2009; 12:312–336. [PubMed: 20067707]

Balzarini J, Pannecouque C, De Clercq E, Aquaro S, Perno CF, Egberink H, Holy A. Antiretrovirus activity of a novel class of acyclic pyrimidine nucleoside phosphonates. Antimicrob Agents Chemother. 2002; 46:2185–2193. [PubMed: 12069973]

Bao H, Li L, Zhang H. Influence of cetyltrimethylammonium bromide on physicochemical properties and microstructures of chitosan-TPP nanoparticles in aqueous solutions. J Colloid Interface Sci. 2008; 328:270–277. [PubMed: 18840381]

Bei D, Marszalek J, Youan BB. Formulation of dacarbazine-loaded Cubosomes--part II: influence of process parameters. AAPS PharmSciTech. 2009a; 10:1040–1047. [PubMed: 19688599]

Bei D, Marszalek J, Youan BB. Formulation of dacarbazine-loaded cubosomes-part I: influence of formulation variables. AAPS PharmSciTech. 2009b; 10:1032–1039. [PubMed: 19669896]

Bhatt DC, Dhake AS, Khar RK, Mishra DN. Development and in-vitro evaluation of transdermal matrix films of metoprolol tartrate. Yakugaku Zasshi. 2008; 128:1325–1331. [PubMed: 18758147]

Bravo-Osuna I, Vauthier C, Farabollini A, Palmieri GF, Ponchel G. Mucoadhesion mechanism of chitosan and thiolated chitosan-poly(isobutyl cyanoacrylate) core-shell nanoparticles. Biomaterials. 2007; 28:2233–2243. [PubMed: 17261330]

Calvo P, Remunan-Lopez C, Vila-Jato JL, Alonso MJ. Chitosan and chitosan/ethylene oxide-propylene oxide block copolymer nanoparticles as novel carriers for proteins and vaccines. Pharm Res. 1997; 14:1431–1436. [PubMed: 9358557]

Cordova M, Cheng M, Trejo J, Johnson SJ, Willhite GP, Liang JT, Berkland C. Delayed HPAM gelation via transient sequestration of chromium in polyelectrolyte complex nanoparticles. Macromolecules. 2008; 41:4398–4404.

Costa P, Sousa Lobo JM. Modeling and comparison of dissolution profiles. Eur J Pharm Sci. 2001; 13:123–133. [PubMed: 11297896]

das Neves J, Amiji M, Sarmento B. Mucoadhesive nanosystems for vaginal microbicide development: friend or foe? Wiley Interdiscip Rev Nanomed Nanobiotechnol. 2011 DOI: 10.1002/wnan.144.

De Campos AM, Sanchez A, Gref R, Calvo P, Alonso MJ. The effect of a PEG versus a chitosan coating on the interaction of drug colloidal carriers with the ocular mucosa. Eur J Pharm Sci. 2003; 20:73–81. [PubMed: 13678795]

Denkba ED, Seyyalb M, Pikin E. Implantable 5-fluorouracil loaded chitosan scaffolds prepared by wet spinning. Journal of Membrane Science. 2000; 172:33–38.

Duan J, Zhang Y, Han S, Chen Y, Li B, Liao M, Chen W, Deng X, Zhao J, Huang B. Synthesis and in vitro/in vivo anti-cancer evaluation of curcumin-loaded chitosan/poly(butyl cyanoacrylate) nanoparticles. Int J Pharm. 2010

Dudhania A, Kosaraju S. Bioadhesive chitosan nanoparticles: Preparation and characterization. Carbohydrate Polymers. 2010; 81:243–251.

Fernandez-Urrusuno R, Calvo P, Remunan-Lopez C, Vila-Jato JL, Alonso MJ. Enhancement of nasal absorption of insulin using chitosan nanoparticles. Pharm Res. 1999; 16:1576–1581. [PubMed: 10554100]

Ghaderi R, Carlfors J. Biological activity of lysozyme after entrapment in poly(d,l-lactide-co-glycolide)-microspheres. Pharm Res. 1997; 14:1556–1562. [PubMed: 9434274]

Grabovac V, Guggi D, Bernkop-Schnurch A. Comparison of the mucoadhesive properties of various polymers. Adv Drug Deliv Rev. 2005; 57:1713–1723. [PubMed: 16183163]

Grayson AC, Doody AM, Putnam D. Biophysical and structural characterization of polyethylenimine-mediated siRNA delivery in vitro. Pharm Res. 2006; 23:1868–1876. [PubMed: 16845585]

Grim SA, Romanelli F. Tenofovir disoproxil fumarate. Ann Pharmacother. 2003; 37:849–859. [PubMed: 12773076]

Hamidi M, Azadi A, Rafiei P. Hydrogel nanoparticles in drug delivery. Adv Drug Deliv Rev. 2008; 60:1638–1649. [PubMed: 18840488]

Hu M, Li Y, Decker EA, Xiao H, McClements DJ. Influence of tripolyphosphate cross-linking on the physical stability and lipase digestibility of chitosan-coated lipid droplets. J Agric Food Chem. 2010; 58:1283–1289. [PubMed: 19921835]

Ikinci G, Senel S, Akincibay H, Kas S, Ercis S, Wilson CG, Hincal AA. Effect of chitosan on a periodontal pathogen Porphyromonas gingivalis. Int J Pharm. 2002; 235:121–127. [PubMed: 11879747]

Jackson SJ, Perkins AC. In vitro assessment of the mucoadhesion of cholestyramine to porcine and human gastric mucosa. Eur J Pharm Biopharm. 2001; 52:121–127. [PubMed: 11522476]

Johnson TJ, Gupta KM, Fabian J, Albright TH, Kiser PF. Segmented polyurethane intravaginal rings for the sustained combined delivery of antiretroviral agents dapivirine and tenofovir. Eur J Pharm Sci. 2010; 39:203–212. [PubMed: 19958831]

Jung T, Kamm W, Breitenbach A, Kaiserling E, Xiao JX, Kissel T. Biodegradable nanoparticles for oral delivery of peptides: is there a role for polymers to affect mucosal uptake? Eur J Pharm Biopharm. 2000; 50:147–160. [PubMed: 10840198]

Klebanoff SJ, Coombs RW. Viricidal effect of Lactobacillus acidophilus on human immunodeficiency virus type 1: possible role in heterosexual transmission. J Exp Med. 1991; 174:289–292. [PubMed: 1647436]

Lackman-Smith C, Osterling C, Luckenbaugh K, Mankowski M, Snyder B, Lewis G, Paull J, Profy A, Ptak RG, Buckheit RW Jr, Watson KM, Cummins JE Jr, Sanders-Beer BE. Development of a comprehensive human immunodeficiency virus type 1 screening algorithm for discovery and preclinical testing of topical microbicides. Antimicrob Agents Chemother. 2008; 52:1768–1781. [PubMed: 18316528]

Leane MM, Nankervis R, Smith A, Illum L. Use of the ninhydrin assay to measure the release of chitosan from oral solid dosage forms. Int J Pharm. 2004; 271:241–249. [PubMed: 15129991]

Lide DR. 2009–2010.

Ma L, Liu C. Preparation of chitosan microspheres by ionotropic gelation under a high voltage electrostatic field for protein delivery. Colloids Surf B Biointerfaces. 2010; 75:448–453. [PubMed: 19819676]

Ma Z, Lim LY. Uptake of chitosan and associated insulin in Caco-2 cell monolayers: a comparison between chitosan molecules and chitosan nanoparticles. Pharm Res. 2003; 20:1812–1819. [PubMed: 14661926]

Miller, JC.; Miller, JN. Statistics for Analytical Chemistry. 3 ed. New York: Ellis Horwood; 1993.

Mohammadpourdounighi N, Behfar A, Ezabadi A, Zolfagharian H, Heydari M. Preparation of chitosan nanoparticles containing Naja naja oxiana snake venom. Nanomedicine. 2010; 6:137–143. [PubMed: 19616121]

Nasti A, Zaki NM, de Leonardis P, Ungphaiboon S, Sansongsak P, Rimoli MG, Tirelli N. Chitosan/TPP and chitosan/TPP-hyaluronic acid nanoparticles: systematic optimisation of the preparative process and preliminary biological evaluation. Pharm Res. 2009; 26:1918–1930. [PubMed: 19507009]

Owen DH, Katz DF. A vaginal fluid simulant. Contraception. 1999; 59:91–95. [PubMed: 10361623]

Pandey R, Ahmad Z, Sharma S, Khuller GK. Nano-encapsulation of azole antifungals: potential applications to improve oral drug delivery. Int J Pharm. 2005; 301:268–276. [PubMed: 16023808]

Park JH, Saravanakumar G, Kim K, Kwon IC. Targeted delivery of low molecular drugs using chitosan and its derivatives. Adv Drug Deliv Rev. 2010; 62:28–41. [PubMed: 19874862]

Parveen S, Mitra M, Krishnakumar S, Sahoo SK. Enhanced antiproliferative activity of carboplatin-loaded chitosan-alginate nanoparticles in a retinoblastoma cell line. Acta Biomater. 2010; 6:3120–3131. [PubMed: 20149903]

Plapied L, Vandermeulen G, Vroman B, Preat V, des Rieux A. Bioadhesive nanoparticles of fungal chitosan for oral DNA delivery. Int J Pharm. 2010; 398:210–218. [PubMed: 20674728]

Quayle AJ. The innate and early immune response to pathogen challenge in the female genital tract and the pivotal role of epithelial cells. J Reprod Immunol. 2002; 57:61–79. [PubMed: 12385834]

Rohan LC, Moncla BJ, Kunjara Na Ayudhya RP, Cost M, Huang Y, Gai F, Billitto N, Lynam JD, Pryke K, Graebing P, Hopkins N, Rooney JF, Friend D, Dezzutti CS. In vitro and ex vivo testing of tenofovir shows it is effective as an HIV-1 microbicide. PLoS One 5. 2010:e9310.

Sano M, Hosoya O, Takao S, Seki T, Kawaguchi T, Sugibayashi K, Juni K, Morimoto Y. Relationship between Solubility of Chitosan in Alcoholic Solution and Its Gelation. Chemical and pharmaceutical bulletin. 1999; 47:1044–1046.

Sassi AB, Isaacs CE, Moncla BJ, Gupta P, Hillier SL, Rohan LC. Effects of physiological fluids on physical-chemical characteristics and activity of topical vaginal microbicide products. J Pharm Sci. 2008; 97:3123–3139. [PubMed: 17922539]

Sayin B, Somavarapu S, Li XW, Sesardic D, Senel S, Alpar OH. TMC-MCC (N-trimethyl chitosan-mono-N-carboxymethyl chitosan) nanocomplexes for mucosal delivery of vaccines. Eur J Pharm Sci. 2009; 38:362–369. [PubMed: 19733658]

Songsurang K, Praphairaksit N, Siraleartmukul K, Muangsin N. Electrospray fabrication of doxorubicin-chitosan-tripolyphosphate nanoparticles for delivery of doxorubicin. Arch Pharm Res. 2011; 34:583–592. [PubMed: 21544723]

Squier CA, Mantz MJ, Schlievert PM, Davis CC. Porcine vagina ex vivo as a model for studying permeability and pathogenesis in mucosa. J Pharm Sci. 2008; 97:9–21. [PubMed: 17721937]

Sun W, Mao S, Wang Y, Junyaprasert VB, Zhang T, Na L, Wang J. Bioadhesion and oral absorption of enoxaparin nanocomplexes. Int J Pharm. 2010; 386:275–281. [PubMed: 19958824]

Tadros T, Izquierdo P, Esquena J, Solans C. Formation and stability of nano-emulsions. Adv Colloid Interface Sci. 2004; 108–109:303–318.

Thongborisute J, Takeuchi H, Yamamoto H, Kawashima Y. Visualization of the penetrative and mucoadhesive properties of chitosan and chitosan-coated liposomes through the rat intestine. J Liposome Res. 2006; 16:127–141. [PubMed: 16753967]

Tiyaboonchai W, Limpeanchob N. Formulation and characterization of amphotericin B-chitosan-dextran sulfate nanoparticles. Int J Pharm. 2007; 329:142–149. [PubMed: 17000065]

Tobyna M, Johnsona J, Dettmar P. Factors affecting in vitro gastric mucoadhesion IV. Influence of tablet excipients, surfactants and salts on the observed mucoadhesion of polymers. European Journal of Pharmaceutics and Biopharmaceutics. 1997; 43:65–71.

Van Gelder J, Witvrouw M, Pannecouque C, Henson G, Bridger G, Naesens L, De Clercq E, Annaert P, Shafiee M, Van den Mooter G, Kinget R, Augustijns P. Evaluation of the potential of ion pair formation to improve the oral absorption of two potent antiviral compounds, AMD3100 and PMPA. Int J Pharm. 1999; 186:127–136. [PubMed: 10486430]

Vander Heyden Y, Nijhuis A, Smeyers-Verbeke J, Vandeginste BG, Massart DL. Guidance for robustness/ruggedness tests in method validation. J Pharm Biomed Anal. 2001; 24:723–753. [PubMed: 11248467]

Vllasaliu D, Exposito-Harris R, Heras A, Casettari L, Garnett M, Illum L, Stolnik S. Tight junction modulation by chitosan nanoparticles: Comparison with chitosan solution. Int J Pharm. 2010

Wiegand C, Winter D, Hipler UC. Molecular-weight-dependent toxic effects of chitosans on the human keratinocyte cell line HaCaT. Skin Pharmacol Physiol. 2010; 23:164–170. [PubMed: 20110767]

Wilks M, Wiggins R, Whiley A, Hennessy E, Warwick S, Porter H, Corfield A, Millar M. Identification and H(2)O(2) production of vaginal lactobacilli from pregnant women at high risk of preterm birth and relation with outcome. J Clin Microbiol. 2004; 42:713–717. [PubMed: 14766841]

Woodrow KA, Cu Y, Booth CJ, Saucier-Sawyer JK, Wood MJ, Saltzman WM. Intravaginal gene silencing using biodegradable polymer nanoparticles densely loaded with small-interfering RNA. Nat Mater. 2009; 8:526–533. [PubMed: 19404239]

Wu Y, Wang Y, Luo G, Dai Y. In situ preparation of magnetic Fe3O4-chitosan nanoparticles for lipase immobilization by cross-linking and oxidation in aqueous solution. Bioresour Technol. 2009; 100:3459–3464. [PubMed: 19329306]

Wu Y, Yang W, Wang C, Hu J, Fu S. Chitosan nanoparticles as a novel delivery system for ammonium glycyrrhizinate. Int J Pharm. 2005; 295:235–245. [PubMed: 15848008]

Yu CY, Cao H, Zhang XC, Zhou FZ, Cheng SX, Zhang XZ, Zhuo RX. Hybrid nanospheres and vesicles based on pectin as drug carriers. Langmuir. 2009; 25:11720–11726. [PubMed: 19719161]

Zhang S, Kawakami K. One-step preparation of chitosan solid nanoparticles by electrospray deposition. Int J Pharm. 2010; 397:211–217. [PubMed: 20637272]

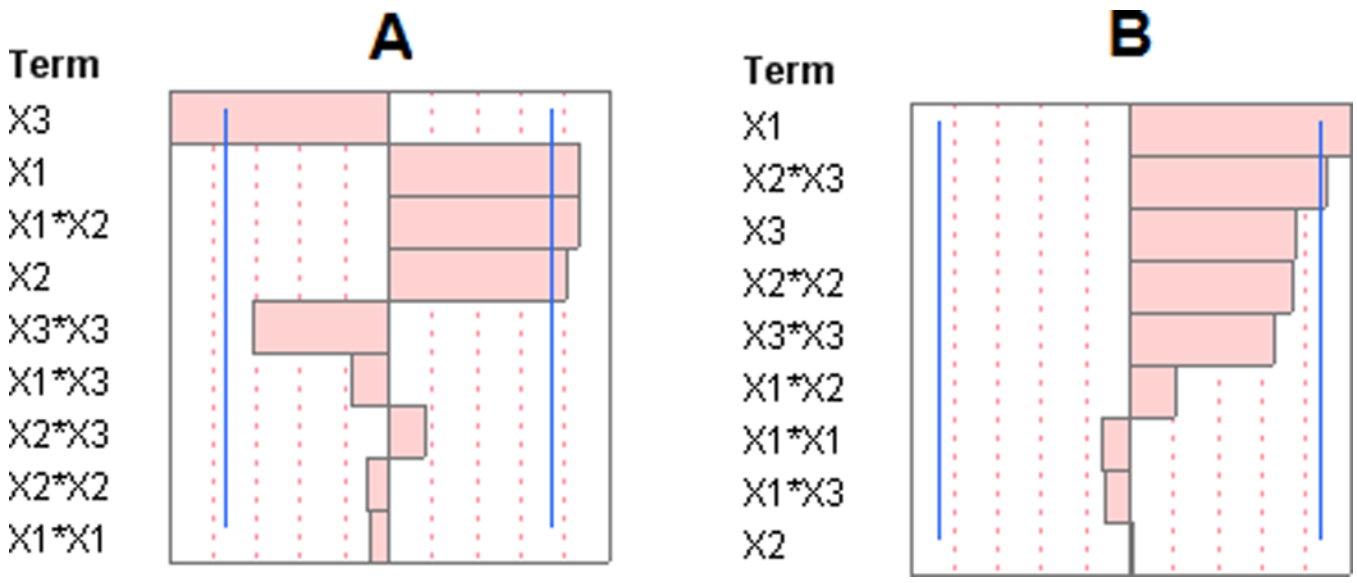

Fig. 1.

Standardized pareto chart for Y_1 (A) and Y_2 (B). Pareto chart showing the standardized effect of formulation variables and their interaction on Y_1 and Y_2. The X-axis shows the t ratio of the variables; bars extending pass the vertical line indicate values reaching statistical significance (α=0.05).

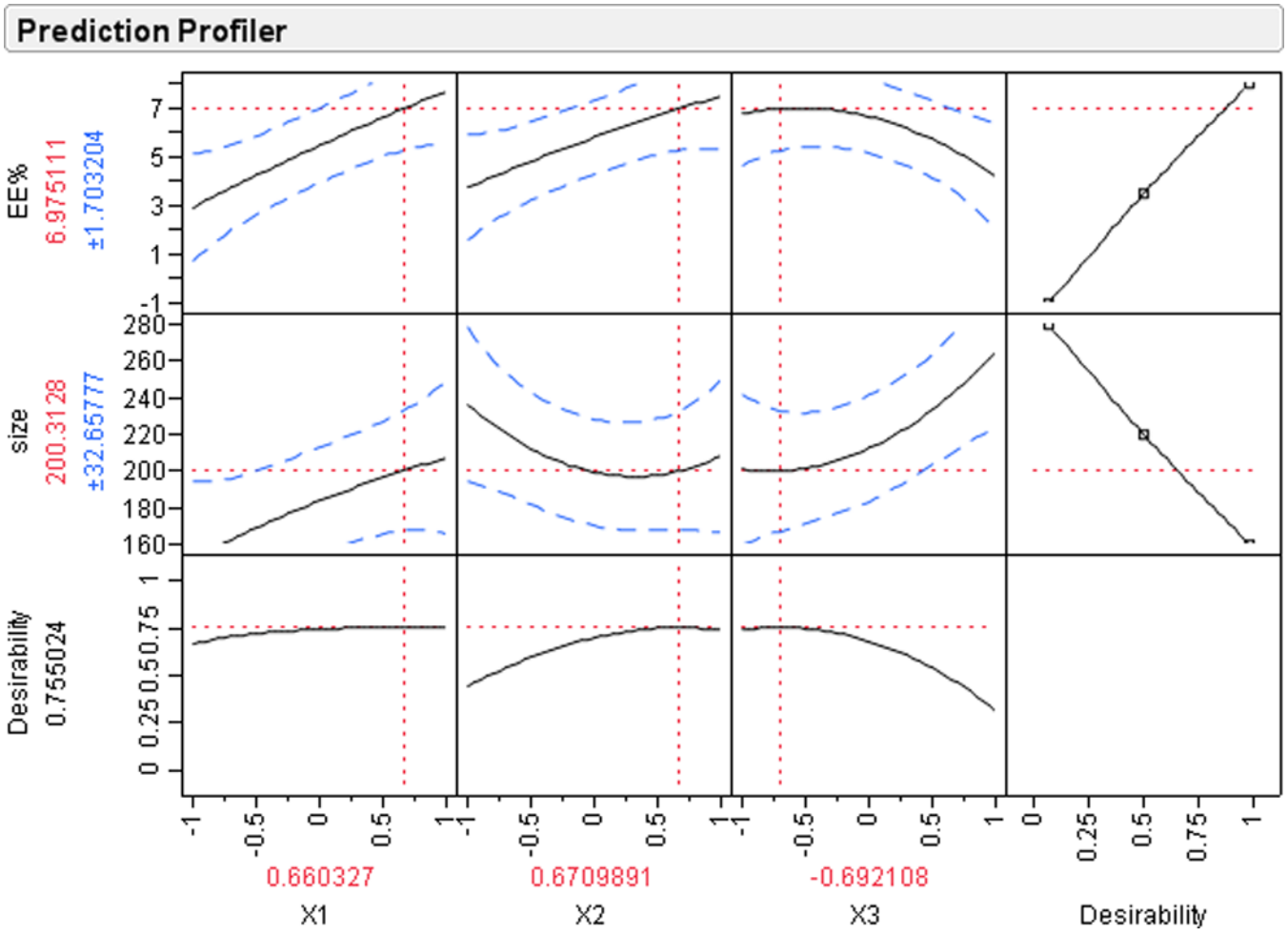

Fig. 2.
Prediction profiler and desirability plot showing the effect of formulation variables on EE% (Y_1) and size (Y_2).

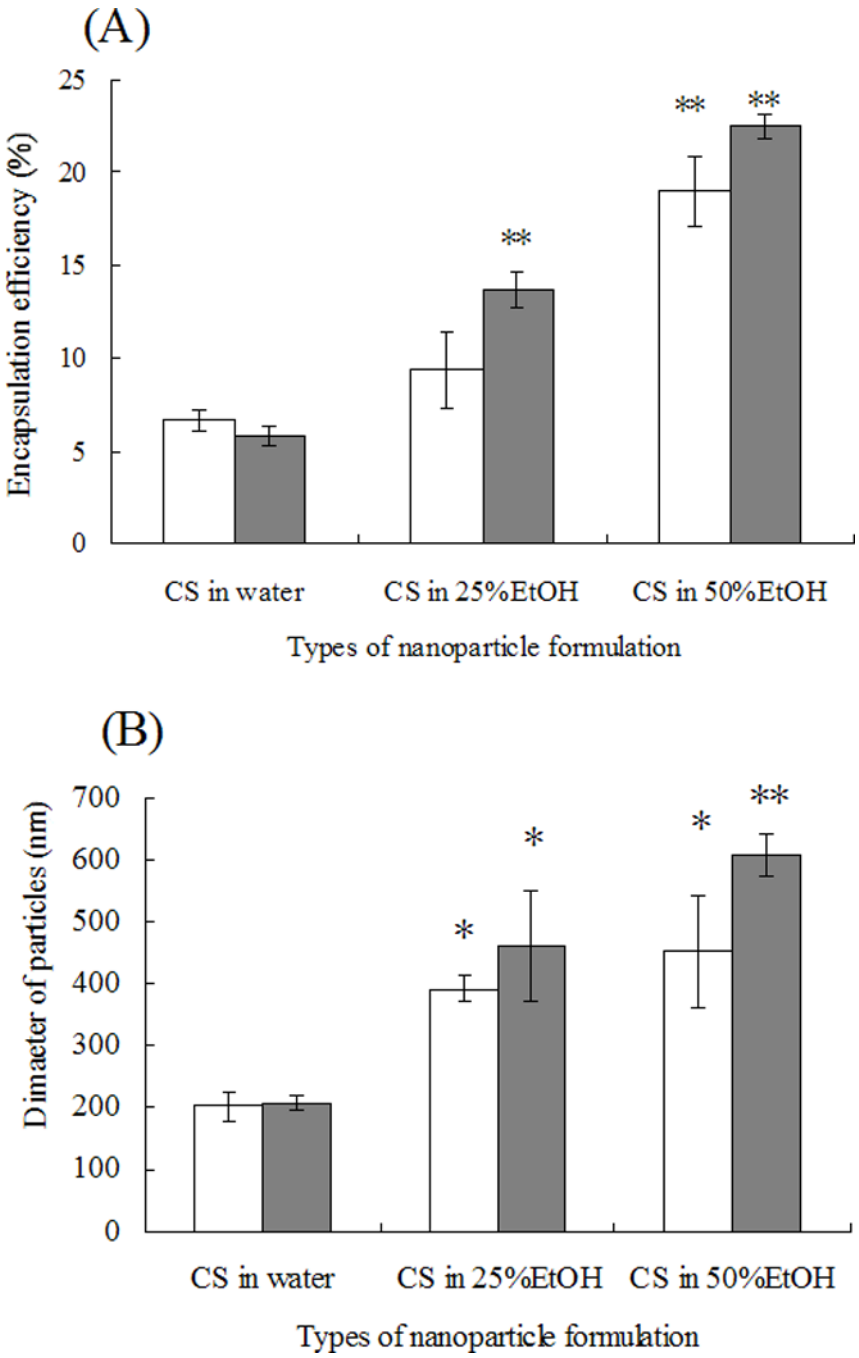

Fig. 3.

EE% (A) and size (B) of NPs that are formed in water and in 50% (v/v) ethanol. □: NPs formed under the conditions from exhibiting the highest EE% among the 15 run (X_1=1, X_2=1, X_3=0); □: NPs formed under the optimal condition (X_1=0.66, X_2=0.67, X_3=−0.69) (n=3). * P<0.05 vs Water, **P<0.01 vs Water

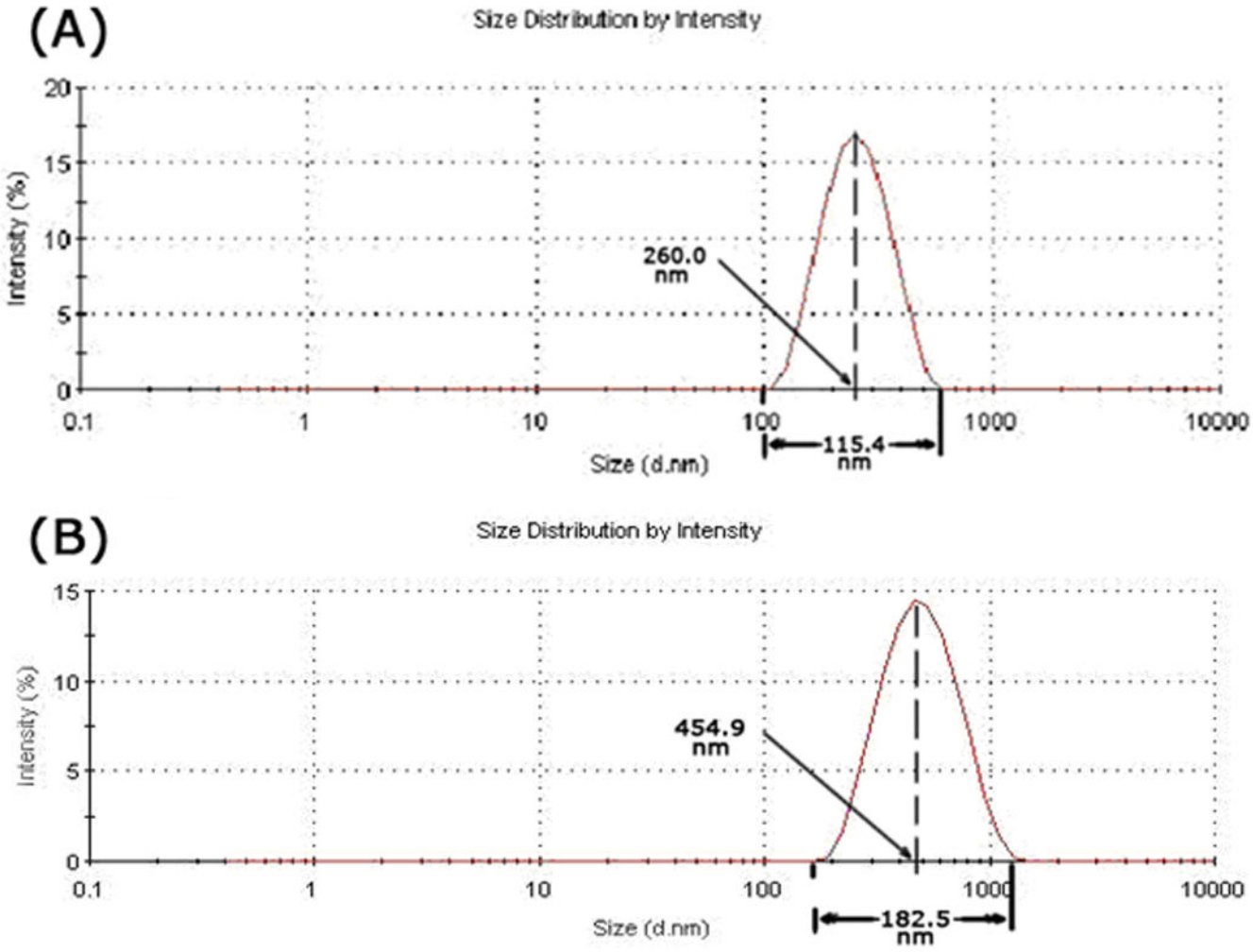

Fig. 4.

Particle size distributions by intensity of chitosan NPs formed in water (A) and in 50% (v/v) ethanol (B).

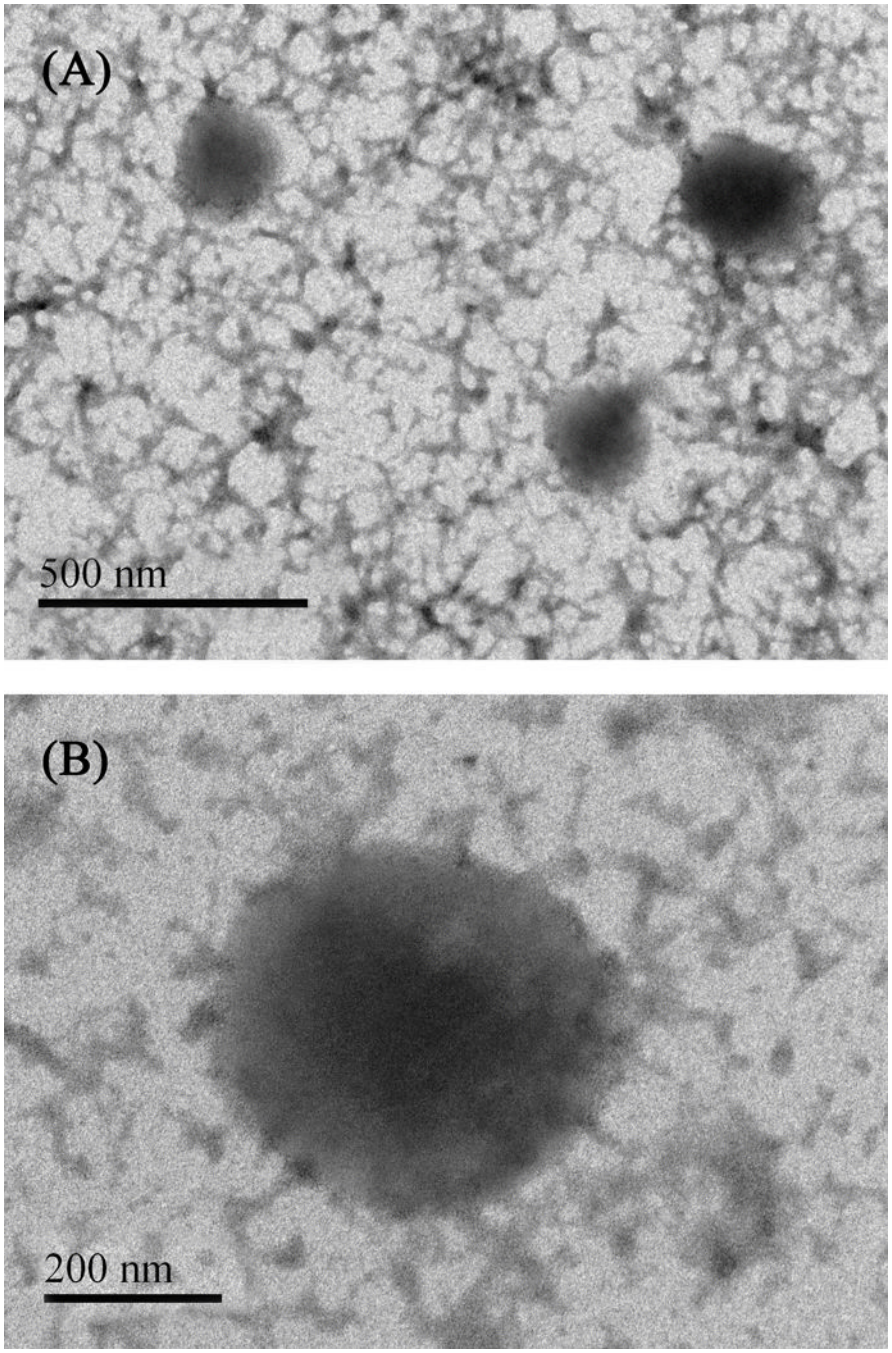

Fig. 5.
Transmission electron microscopy (TEM) of chitosan NPs prepared using water (A) and 50% (v/v) ethanol (B) as the preparation media.

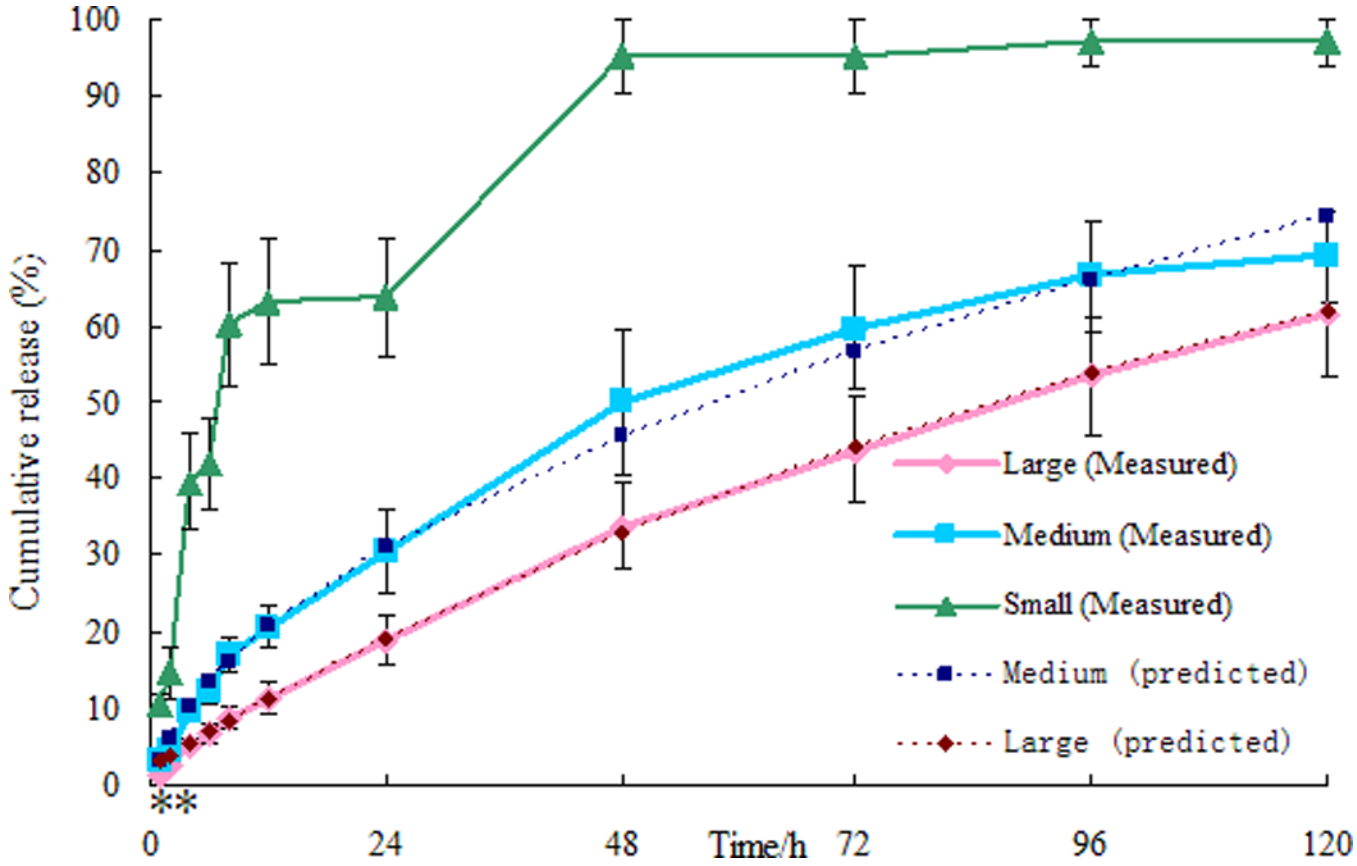

Fig. 6.

In vitro release profiles of chitosan NPs with small, medium and large size (n=3).

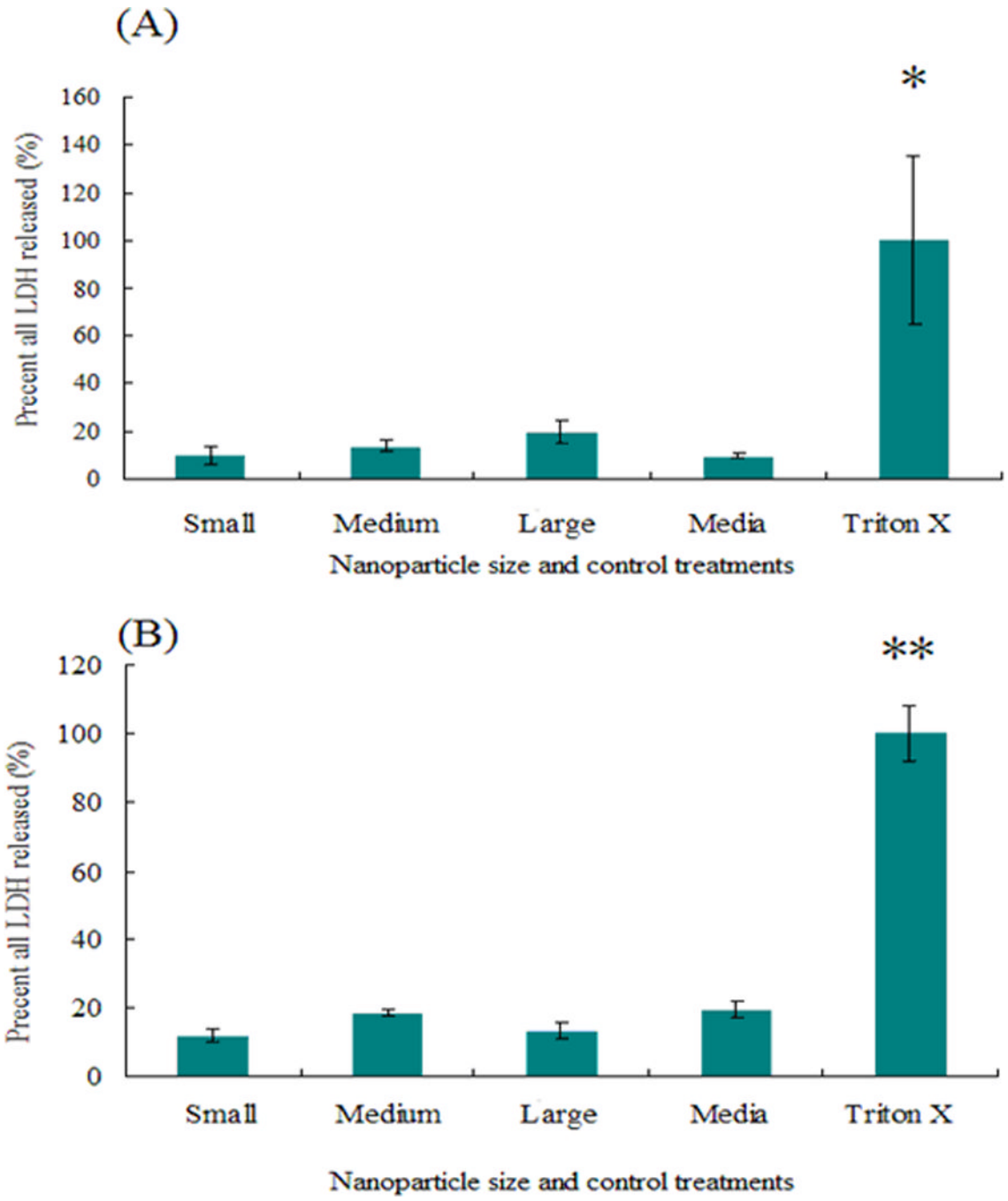

Fig. 7.

LDH release of vaginal epithelial cells treated by chitosan NPs with different sizes for 4 hours (A) and 48 hours (B), (n=3). * $P<0.05$ vs Media, ** $P<0.01$ vs Media

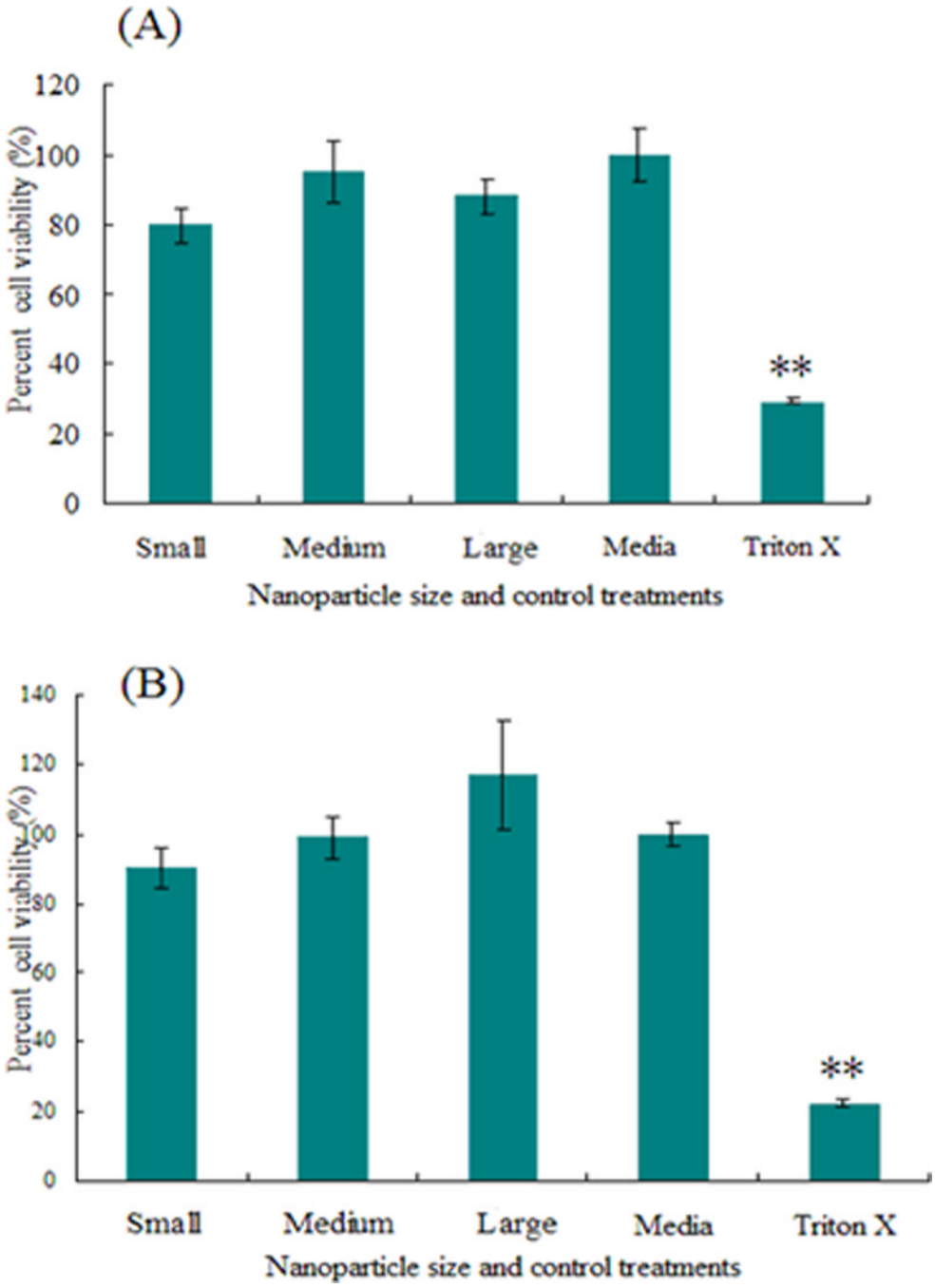

Fig. 8.

Percent viability of vaginal epithelial cells treated by chitosan NPs with different sizes for 4 hours (A) and 48 hours (B), (n=3). * $P<0.05$ vs Media, ** $P<0.01$ vs Media

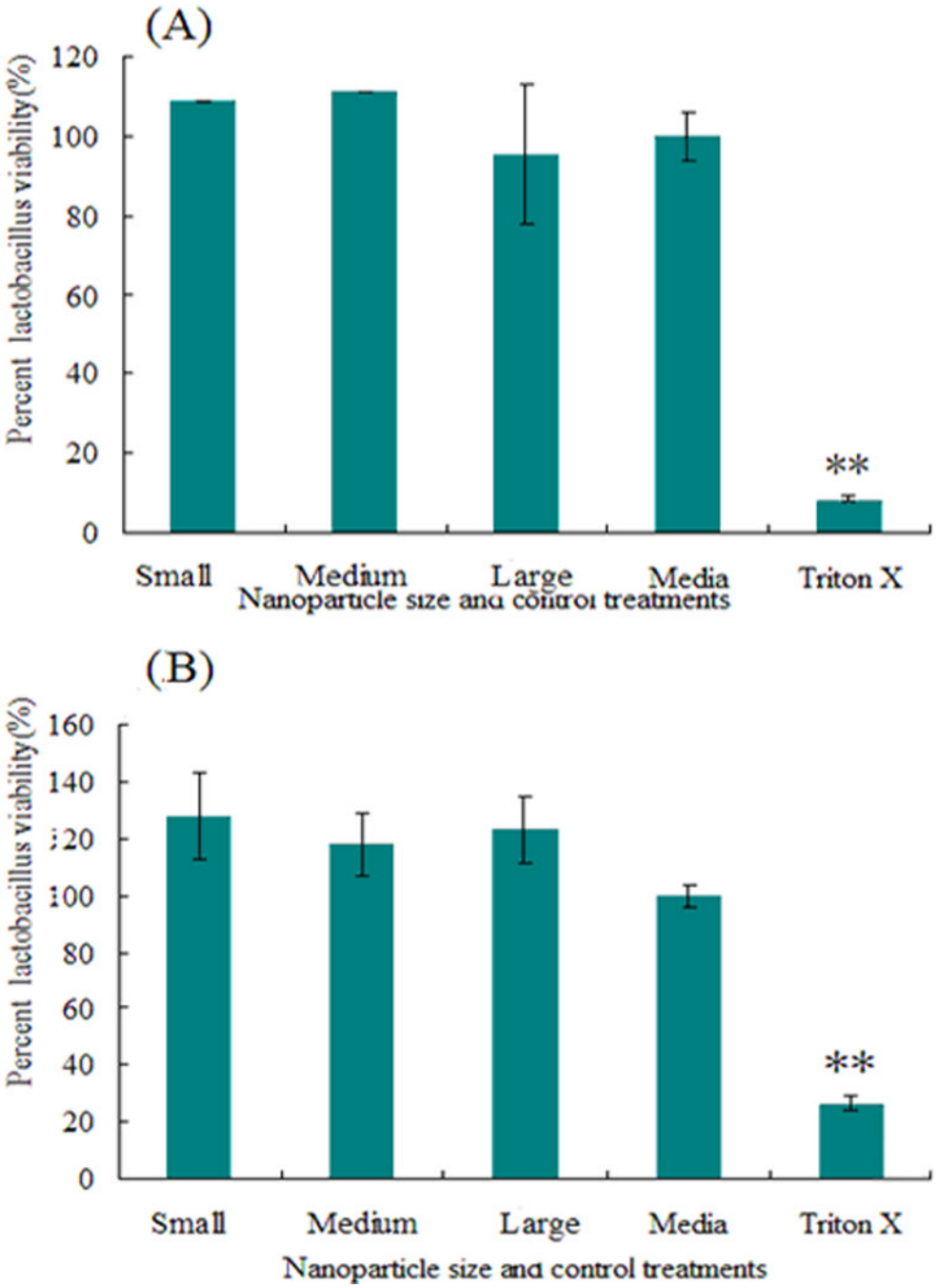

Fig. 9.

Percent viability of *Lactobacillus cripatus* treated by chitosan NPs with different sizes for 4 hours (a) and 48 hours (b), (n=3). * P<0.05 vs Media, **P<0.01 vs Media

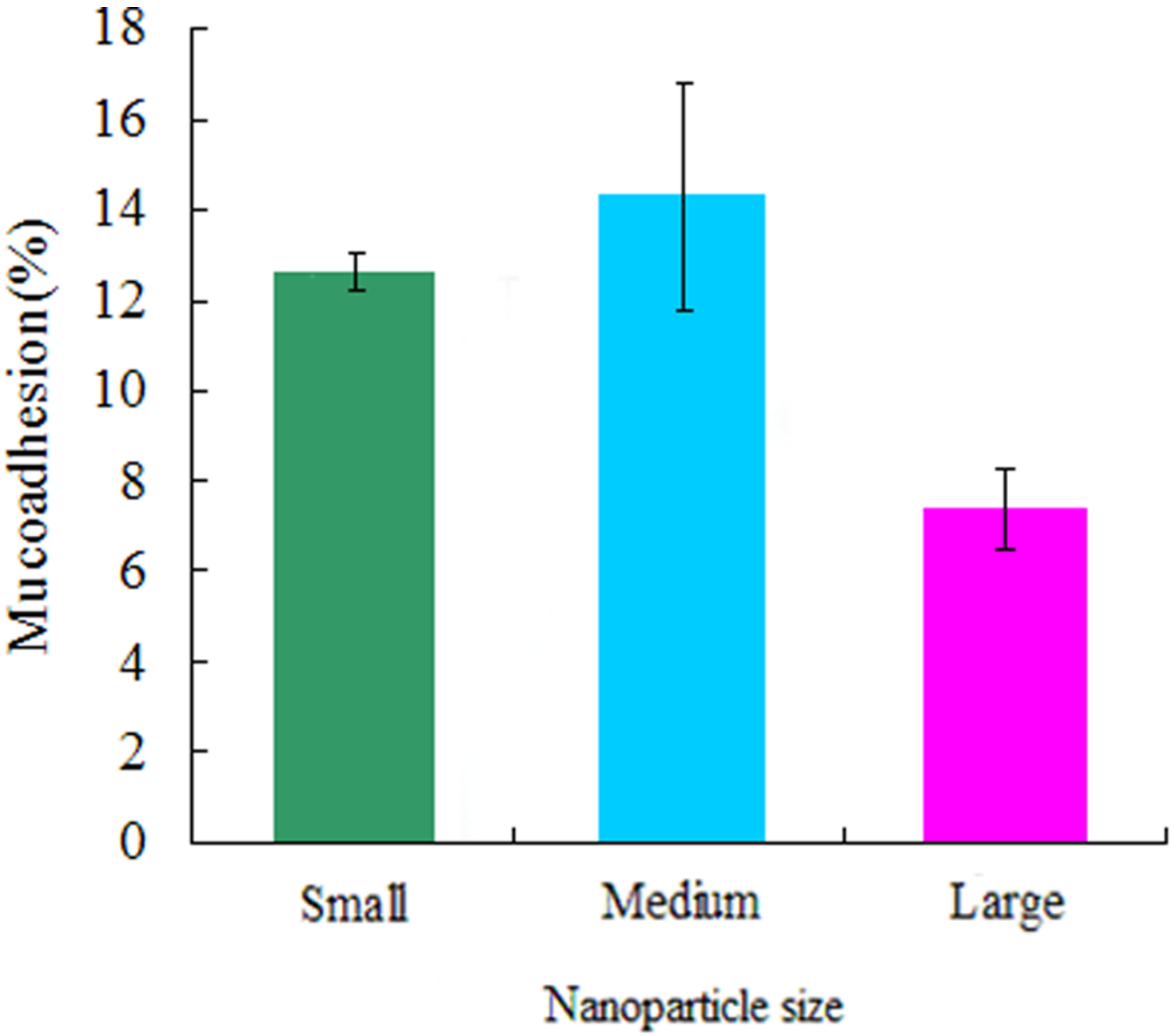

Fig. 10.

Percent mucoadhesion of chitosan particles with different sizes on porcine vaginal tissue. After fluorescence labeling, the mean diameters of small, medium, and large particles were 188.7±43.3 nm, 273.5±53.1 nm, and 900.2±118.4 nm, respectively for n=3.

Table 1

Independent variables and their levels in Box-behnken design

Independent variables	Low	Medium	High
X_1= concentration of chitosan (w/v %)[a]	0.1	0.2	0.3
X_2=TPP/chitosan (w/w)	0.1	0.2	0.3
X_3=drug/chitosan (w/w)	0.1	0.2	0.3
Coded values	−1	0	1
Dependent values			
Y_1= encapsulation efficiency (EE)%			
Y_2= size (nm)			

[a]The volume of chitosan was 10 ml

Table 2

Box-Behenken experimental design showing independent variables with measured responses

Model	X_1	X_2	X_3	Y_1	PI	Y_2
−−0	−1	−1	0	4.47	0.307	174.1
−0−	−1	0	−1	2.07	0.316	183
−0+	−1	0	1	1.23	0.436	209.1
−+0	−1	1	0	3.11	0.227	168.5
0−−	0	−1	−1	4.25	0.284	238
0−+	0	−1	1	0	0.272	228.2
000	0	0	0	4.57	0.411	196
000	0	0	0	5.09	0.226	188.2
000	0	0	0	4.33	0.236	176.8
0+−	0	1	−1	6.04	0.272	179.1
0++	0	1	1	2.98	0.319	277
+−0	1	−1	0	2.42	0.248	231.3
+0−	1	0	−1	6.07	0.249	204.5
+0+	1	0	1	3.98	0.306	217.8
++0	1	1	0	7.33	0.428	250.1

Eur J Pharm Sci. Author manuscript; available in PMC 2012 June 14.

Table 3

ANOVA analysis for both measured responses.

Response	Source	DF[a]	SS[b]	MS[c]	F ratio[d]	P value
Y_1	Model	9	47.376	5.26	4.77	0.049
	Error	5	5.50	1.10		
	Total	14	52.88			
Y_2	Model	9	12147.75	1349.75	3.33	0.099
	Error	5	2025.05	405.01		
	Total	14	14172.80			

[a] degree of freedom,

[b] sum of square,

[c] mean sum of square,

[d] Model MS/error MS

Table 4

Checkpoint experiments comparing measured and predicted responses (n=3).

Run no.	X_1	X_2	X_3	Measured Y_1	Predicted Y_1	Error% forY_1	P Value for Y_1	Measured Y_2	Predicted Y_2	Error% of Y_2	P Value for Y_2
C1	−0.5	−0.5	−0.5	5.55 (±1.82)	4.24	30.90	0.34	166.23 (±16.05)	185.63	−10.45	0.17
C2	0.5	0.5	0.5	3.18 (±1.44)	5.11	−42.70	0.15	266.33 (±85.84)	223.08	20.73	0.47
C3	0.66	0.67	−0.69	5.83 (±0.88)	6.97	−16.36	0.15	207.97 (±19.07)	200.31	3.82	0.56

Table 5

Physico-chemical properties of NPs used in drug release and cytotoxicity studies. (n=6)

Size	Formulation				Average particle size (nm)	Zeta potential (mV)	EE %	Drug loading % (w/w)
	X1	X2	X3	Preparation media				
Low	−1	0	−1	water	182.36 (±15.83)	46.4 (±1.22)	2.1 (±0.6)	0.21 (±0.06)
Medium	0.66	0.67	−0.69	water	281.67 (±25.62)	53.07 (±0.56)	6.9 (±0.7)	0.33 (±0.05)
High	0.66	0.67	−0.69	ethanol/water 50/50 (v/v)	602.43 (±48.96)	55.23 (±2.29)	23.5 (±1.2)	1.14 (±0.06)